Thermal Rate Constant for CN + H_2/D_2 → HCN/DCN + H/D Reaction from T = 293 to 380 K

G. He, I. Tokue,† and R. Glen Macdonald*

Argonne National Laboratory, Chemistry Division, 9700 South Cass Ave., Argonne, Illinois 60565

Received: January 23, 1998; In Final Form: April 16, 1998

The reaction rate constant for the cyano (CN) radical with hydrogen and deuterium has been determined over the temperature range 293−380 K. The CN radical was detected by time-resolved near-infrared absorption using the CN red system ($A^2\Pi \leftarrow X^2\Sigma$) (2,0) band near 790 nm. These measurements were carried out at low pressures of Ar or He as carrier gas. The diffusion rate of CN in these mixtures was inferred from the diffusion rate of HCN(000) determined using time-resolved infrared absorption of HCN(000) around 3.0 μm, simultaneously with the detection of CN. These measurements provide accurate thermal rate constant data that will enable a detailed comparison to be made between theoretical predictions and experimental measurements for this prototypical reaction system.

I. Introduction

The reaction of the cyano radical (CN) with H_2

$$CN + H_2 \xrightarrow{k_{R1}} HCN + H \qquad (R1)$$

and its deuterated analogue

$$CN + D_2 \xrightarrow{k_{R2}} DCN + D \qquad (R2)$$

are ideal systems to study the reaction dynamics of four-atom systems.[1] Over the past decade or so there has been an increasing effort both experimentally and theoretically to probe this system from a variety of perspectives. An important experimental aspect of this problem is the determination of accurate thermal rate constants[2] for reactions R1 and R2, and from the theoretical point of view, it is important to develop a global potential energy surface (PES). This PES should describe all the possible interactions that can occur in the four-atom H−H−C−N system, i.e., the intermediates H_2CN and HCNH and both product channels, HCN + H and HNC + H. Such a global PES has recently been developed for reaction R1 based on accurate ab initio calculations of over 12 000 points in the H−H−C−N configuration space.[3] The temperature dependence of the thermal rate constant was calculated using a quasiclassical trajectory approach that completely accounted for the six degrees of internal motion of the four-atom system on this global PES. The barrier height was adjusted from the ab initio value of 4.3 kcal mol^{-1} to 3.2 kcal mol^{-1} in order to obtain agreement with the average rate constant data for reaction R1 at 300 K. The value of k_{R1} over the temperature range 200−3500 K was then calculated and found to in good agreement with experiment. This value for the barrier height for reaction R2 was also suggested by Che and Liu[4] from the determination of the excitation function for reaction R2 in a molecular beam. In a recent work Wang et al.[5] again compared very detailed molecular beam experiments with predictions from quasiclassical trajectory calculations, again based on the recent global surface. They also suggested that the surface could be modified to obtain better agreement between theory and experiment.

Earlier theoretical analysis of reaction R1 by Wagner and Bair[6] also used a comparison of theoretical rate constants for reaction R1 and experimental values to refine the properties of the transition state for the abstraction channel. These workers carried out a detailed analysis of the saddle point properties for reaction R1 using an ab initio generalized valence bond configurational interaction (GVB-CI) and more refined calculations for the energetics of the reaction using a POL-CI calculation. Using the theoretical predictions for the transition-state structure, the temperature dependence of k_{R1} was calculated using conventional transition-state theory. Good agreement with experiment was obtained if the theoretically predicted barrier height of 6.0 kcal mol^{-1} was reduced to 4.1 kcal mol^{-1}.

Although there are several recent studies[7−10] of reactions R1 and R2 over wide temperature ranges, there still appears to be some uncertainty as to the value of (R1) around room temperature.[7−13] In light of the recent interest in adjusting the new global PES according to the observed 300 K rate constant data,[3] it was felt that a new determination of the rate constant for reactions R1 and R2 would be worthwhile. Furthermore, most recent[7−10,12] measurements of k_{R1} and/or k_{R2} at low temperatures have been based on pulsed laser-induced fluorescence (LIF) of CN using the violet system, $B^2\Sigma^- \leftarrow X^2\Sigma^+$ (0−0), transition around 380 nm. In these measurements, the time evolution of the CN radical was followed by varying the time delay of the probe LIF laser following the pulsed laser production of the CN radical from a suitable precursor. This method is quite sensitive but requires very careful normalization of pulsed laser intensities. Balla and Pasternack[13] monitored the CN radical continuously using time-resolved infrared absorption of the fundamental CN(v=1;J') ← (v=0;J'') transition near 5.2 μm using a tunable infrared lead salt laser spectrometer. Although this is a direct method for detecting single rovibrational levels of CN in a continuous fashion, the infrared transition dipole moment of CN is small, and this method suffers from a lack of sensitivity. Other approaches have been used to detect the CN radical in a continuous time-resolved fashion,

† Department of Chemistry, Niigata University, Faculty of Science, Niigata 950-21, Japan.

S1089-5639(98)00875-5 CCC: $15.00
Published on Web 05/22/1998

but they have not been applied to the determination of k_{R1} or k_{R2}. Durant and Tully[14] used a high-resolution continuous wave (CW) ultraviolet dye laser to excite LIF of CN using the CN $B^2\Sigma^- \leftarrow X^2\Sigma^+$ (0−0) transition. Recently, Hall and Wu[15] detected CN in a continuous fashion using time-resolved absorption on the CN red system, $A^2\Pi \leftarrow X^2\Sigma^+$ (2−0) band, near 790 nm. This detection scheme was based on a high-resolution tunable CW Ti−sapphire laser spectrometer. North et al.[16] have extended this technique to include time-resolved FM-modulated absorption spectroscopy and applied this technique to a direct kinetic measurement of the reaction rate constant for $CN + C_2H_4$.

In the present work, CN was detected in a continuous fashion using direct absorption of CN on the $A^2\Pi \leftarrow X^2\Sigma^+$ (2−0) transition at 790 nm. The laser source was a commercial external cavity diode laser which has the advantage of narrow bandwidth and tunability combined with low-amplitude fluctuation noise. The sensitivity of the direct absorption technique was improved by multipass optics to increase the absorption path length. The CN radical was created by pulsed laser photolysis of $(CN)_2$ at 193 nm, and its time evolution was followed in low-pressure mixtures of H_2 or D_2 in inert gases to determine k_{R1} and k_{R2}.

II. Experimental Section

The basic experimental apparatus has been described in previous works.[17,18] Briefly, the transverse flow reactor (TFR) consists of a stainless steel chamber which contains a Teflon box of dimensions 100 × 100 × 5 cm. The TFR was evacuated by a liquid nitrogen trapped 25 cfm mechanical pump to a pressure of a few milliTorr. The leak rate of the TFR was less than 1 mTorr/min. To reduce gas consumption and provide a constant pumping speed during an experiment, a small orifice was placed between the mechanical pump and the TFR.

The temperature of the TFR was controlled by circulating hot silicone oil (a NestLab model HT-200 hot oil bath) through copper tubing folded back and forth over the top and bottom surface of the inner Teflon box. Five thermocouples, four of which were inserted in wells in the Teflon box using silicone thermal grease and the fifth was suspended directly in the gas stream, were used to monitor the gas temperature. About 5% of the optical path was in regions not directly heated by the circulating hot oil system. Heating tape was used to heat these side-arm chambers containing the White cell optics to the temperature of the reaction region.

A separate high-vacuum system was used to control the flow of the various gases into the TFR. The Ar, He, and H_2 were all supplied by AGA Gas and were research grade, 99.9995% pure. The D_2 (research grade, 99.5% pure) and $(CN)_2$ (research grade, 98.5% pure) were supplied by Matheson. The $(CN)_2$ was purified by pumping on at −78 °C. The gases were continuously flowed through the TFR and their partial pressures determined from the known flow rates and total pressure in the TFR, as determined by an Edwards model 600 pressure transducer. All except the $(CN)_2$ flow meters were carefully calibrated. In early experiments, calibrated Gilmont rotometers were used to measure the Ar or He and H_2/D_2 flow rates, but at low flow rates of He or H_2 the readings required a long time to stabilize. To overcome this problem, the rotometers were replaced by M.K.S. model 0258 electronic mass flow meters, which were again carefully calibrated.

The CN radical was produced by the photolysis of $(CN)_2$ at 193 nm using a Lumonics model 740 excimer laser. All the experiments were carried out with the photolysis laser power density of 2−10 mJ/cm^2 at a repetition rate of 1−5 Hz. As in previous experiments,[17] the rectangular shaped ArF laser beam propagated through the photolysis region with its long axis perpendicular to the nominal flow direction of the TFR and the split White cell mirror axis.

Single rotational states of the CN radical were detected using time-resolved near-infrared absorption spectroscopy on the CN($A^2\Pi \leftarrow X\ ^2\Sigma^+$) (2,0) band near 790 nm. The room-temperature external cavity diode laser was supplied by Environmental Optical Sensors Inc. This laser reliably runs in a single mode; nevertheless, the mode behavior was monitored by a Burleigh 2 GHz free spectral range scanning Fabry−Perot Etalon. The laser can be continuously tuned over several nanometers without a mode hop. The laser bandwidth was less than 5 MHz, much narrower than the thermal Doppler line width of the CN radical. The laser wavelength was determined using an evacuated Burleigh model IR-210 wavemeter.

White cell optics were used to multipass the probe laser radiation through the photolysis region so that the nominal absorption path length was 14 m. Both the excimer and probe laser radiation were directly overlapped using a dichroic mirror set at Brewster's angle with respect to the probe laser polarization. Another optic, Pyrex or ZnSe, also inserted directly in the optical path at Brewster's angle, was used to absorb the excimer laser radiation and prevent damage to the White cell optics.

The photolysis laser introduced a small instantaneous baseline shift, presumably from a refractive index change induced in one of the optical elements. To account for this, a time-resolved absorption profile was obtained with the probe laser tuned to the peak of an absorption feature, signal averaged for 100−500 shots using a LeCroy model 9410 digital oscilloscope, and then a background profile was recorded and signal averaged with the probe laser frequency detuned several line widths from the peak. These two curves, signal + background and background, were transferred to a laboratory computer and subtracted to produce a time-resolved CN(v=0;J) absorption profile. The reaction rate constants for (R1) and (R2) are small, and the observed first-order exponential decay times ranged from 100 to 5000 s^{-1} so that in order to avoid distortions of these profiles from low-frequency filtering they were collected in a dc mode. As a result, the initial I_0 was recorded simultaneously with the absorption profile using the pretrigger feature of the digital oscilloscope, and the absorbance, $\ln(I_0/I)$, vs time profiles could be directly calculated.

The laser intensity was detected using a New Focus Si PIN photodiode. Care was taken so that the detector was not saturated by the probe laser power. The time response of the Si diode was 100 MHz, but in most of the experiments, the frequency response was limited to the range dc to 3 MHz using a Krohn-Hite model 3944 electronic filter.

The laboratory PC computer that was used to generate the absorbance profiles and data analysis was also used to provide appropriate timing pulses for the data collection sequence and necessary voltages to scan the diode laser.

The apparatus and gas handling system were specifically designed for a flowing gas setup. As a result, the appropriate experimental pressure range was 2−15 Torr; however, at the higher pressures the diffusion rate becomes very slow, and increasing the pumping speed results in rapid consumption of $(CN)_2$ and D_2. Hence, most of the data reported in this work were obtained with a total gas pressure around 4 Torr. At this pressure, diffusion can contribute to the first-order decay rates. To a first-order approximation, the diffusion constant for CN

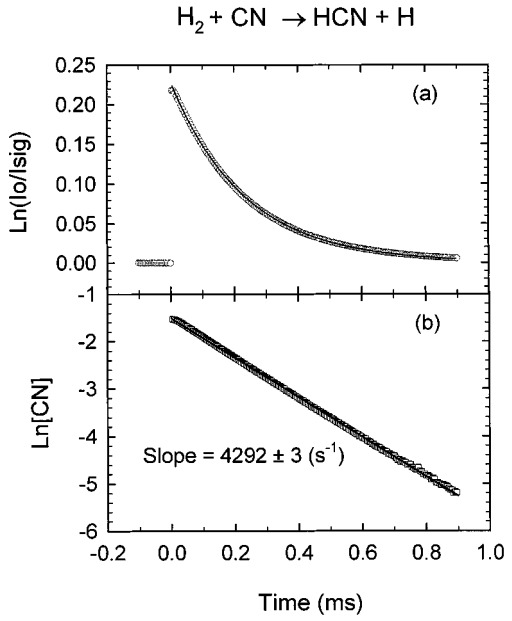

Figure 1. (a) Absorbance of CN(v=0;J=9.5) as a function of time for a temperature of 328 K; P_{H_2} = 3.046, P_{Ar} =1.803, and $P_{(CN)_2}$ = 0.0083 Torr. The solid line is the single-exponential decay fit for the rate determined in Figure 1(b). (b) Determination of k_{CN} for the absorbance profile in Figure 1(a). A linear least-squares fit gives k_{CN} = (4.292 ± 0.003) × 10^3 s^{-1}.

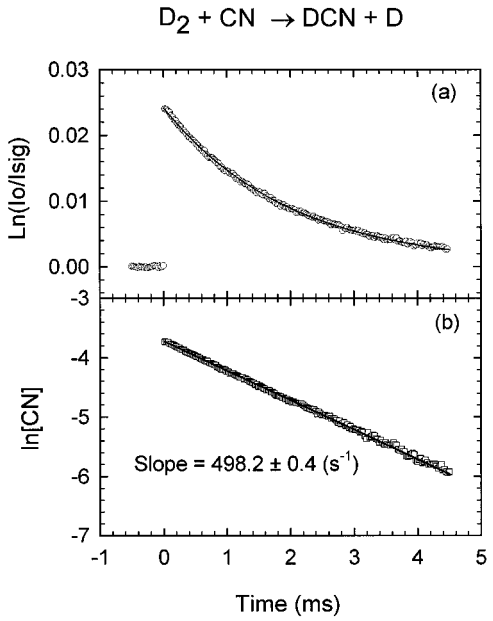

Figure 2. (a) Absorbance of CN(v=0;J=8.5) as a function of time for a temperature of 293 K; P_{D_2} = 0.780, P_{He} = 3.178, and $P_{(CN)_2}$ = 0.0023 Torr. The solid line is the single-exponential decay fit for the rate determined in Figure 2(b). (b) Determination of k_{CN} for the absorbance profile in Figure 2(a). A linear least-squares fit gives k_{CN} = (4.98 ± 0.04) × 10^2 s^{-1}.

and HCN in nonpolar environments should be similar. In this laboratory there is the capability to detect the time dependence of vibrational levels of HCN in the infrared region around 3.0 μm. A Burleigh model FCL-20 single-mode color center laser was used to monitor HCN(000) produced in reaction R1. Both the CN reactant and HCN product could be detected simultaneously. These experiments will be described in detail in another work,[19] but for the present it should be noted that the diffusion rate constants for HCN in mixtures of He−H_2 and Ar−H_2 were measured directly.

III. Results and Discussion

The bandwidth of the probe diode laser radiation was much narrower than the thermal Doppler width of the CN transitions so that the Beer−Lambert law was obeyed, and a plot of absorbance, $A = \ln(I_0/I)$, against time is a direct measure of the temporal concentration profile of CN, [CN] (where the square brackets refer to concentration). At the low initial concentrations of CN used in the present experiments (<7 × 10^{11} molecules cm^{-3}) secondary reactions can be ignored, and the first-order decay of CN, k_{CN} , represents the sum of all removal processes for the CN radicals, i.e., reaction with H_2 or D_2, reaction with any impurities such as O_2 or a hydrocarbon background, and removal by diffusion. To minimize the influence of these possibilities, the first-order removal rates for CN were measured as a function of pressure of H_2 (P_{H_2}) or D_2 at a constant total pressure. Under these circumstances, the second-order rate constant for reaction R1 or R2 can be obtained from the slope of the first-order rates plotted against P_{H_2} or P_{D_2} at constant total pressure. The intercept provides the influence of impurity reactions and diffusion. This treatment assumes of course that the change in reactant partial pressure changes only the reaction rate; however, at low total pressures and especially for Ar as the carrier gas, the diffusion rate constant also depends on gas composition so that the diffusion rate should be subtracted from k_{CN} before plotting the data. The estimates for the diffusion rate of CN in the various mixtures were provided by the direct experimental measurements of diffusion using the HCN(000) measurements.[18,19]

A typical absorbance temporal profile for the removal of CN-(v=0;J=9.5) in H_2−Ar mixtures at a temperature of 328 K is shown in Figure 1a, and the determination of k_{CN} from these data is shown in Figure 1b. A similar absorbance profile for the removal of CN(v=0;J=8.5) in D_2−He mixtures is shown in Figure 2a for a temperature of 293 K, and the determination of k_{CN} from this absorbance trace is shown in Figure 2b. As is evident from Figures 1b and 2b, the data were well described by single-exponential decay rates. This was generally the case for all the data collected in this work, except for low partial pressures of reactants when sometimes the decay curves could be described by two decaying exponential terms. In these cases, the appearance of a second exponential term was likely due to the appearance of multiple diffusion modes.[20] Also, in some cases an induction period, due to rotational relaxation, persisted for several microseconds but was of short enough duration as not to influence the determination of the first-order decay rates.

If the removal of CN by diffusion is described by a single first-order decay rate, k_{CN}^{diff}, at a constant total pressure, then Blanc's law relates[20] the diffusion rate constant to a linear function of the partial pressures of the components in the mixture, i.e.

$$\frac{1}{k_{CN}^{diff}} = \frac{P_{X_2}}{D_{X_2}} + \frac{P_M}{D_M} \qquad (3)$$

where X_2 is either H_2 or D_2, M is either Ar or He, and $D_{X_2,M}$ is the corresponding diffusion coefficient of CN in the pure gas X_2 or M at the pressure $P_{X_2/M}$. With the present geometry the diffusion process was complicated, and at long times (>1 ms) there were two measurable diffusion rate constants, describing five low-order diffusion modes.[20] However, the faster diffusion rate (motion parallel to the short dimension of the rectangular

shaped excimer laser beam) was about 9 times larger than the smaller one (motion parallel to the long dimension). The faster diffusion rate constant was assumed to dominate, and the smaller one was neglected so that the diffusion process could be described by a first-order rate process.

The diffusion process was studied by monitoring HCN(000) at times from 1 to 80 ms following the photolysis laser pulse. At these long times, vibrational relaxation of the whole HCN vibrational manifold was complete as can be inferred from the known vibrational relaxation rate constants of many highly excited HCN levels by H_2[21] and also from experiments carried out in this laboratory.[18] Furthermore, the decay of HCN(001) was observed to be complete before the time scale for diffusion became important. Thus, at these long times the HCN(000) level was proportional to the thermalized HCN product from reaction R1, and its time behavior was not perturbed by vibrational relaxation processes. The diffusion coefficients of CN and HCN should be similar. Virtually all the data for the measurement of k_{R2} were obtained in He−D_2 mixtures for which the diffusion rate for CN should be approximately constant because of the constant effective mass for this gas combination.[22] Simple temperature and mass dependencies predicted by ideal gas kinetic theory were used to extend the determination of the diffusion rate constants to temperatures greater than 294 K and other gas compositions. The majority of the rate constant measurements were made using He as the carrier gas, and k_{CN}^{diff} was almost constant. At most k_{CN}^{diff} varied from 100 to 300 s^{-1} for the CN in the Ar−H_2 mixtures used in this work, and the direct correction for diffusion decreased the measured rate constants by up to 5% for some experiments.

A possible complicating reaction could be the attack of H atoms on $(CN)_2$ to regenerate CN radicals

$$H + (CN)_2 \rightarrow HCN + CN \quad (\Delta H_0 = +41.4 \pm 5.0 \text{ kJ mol}^{-1}) \quad \text{(R3)}$$

where the ΔH_0 has been evaluated from recent data.[23,24] If reaction R3 occurred by a single-step process, then even though the reaction is substantially endothermic, it could become important with increasing temperature if the *A* factor for the rate constant was large. Fortunately, Phillips[25] has studied this reaction at 300 K and found that the rate constant for the disappearance of H atoms was small, $k = 1.5 \times 10^{-15}$ cm^3 $molecule^{-1}$ s^{-1} at a pressure of 1 Torr. These experiments also verified that the mechanism of H atom removal did not occur through reaction R3 but by complicated multistep three-body processes originally proposed by Abers et al.[11] Furthermore, there was no detectable production of CN radicals at long times in the CN + H_2 system so that the influence of this reaction path was negligible.

An important experimental parameter in this reaction system is the temperature. Small uncertainties in the determination of the gas temperature can cause large variations in the observed rate constants because of the relatively large activation barrier for reactions R1 and R2. In principle, the laser photolysis process itself could perturb the gas temperature by depositing energy into the internal degrees of freedom and/or the translational motion of the photolysis products; however, in the present experiments this effect was quite minor. The small absorption cross section of $(CN)_2$ at 193 nm (1.1×10^{-19} cm^2)[13] and low partial pressures of $(CN)_2$ ($P_{(CN)_2} < 0.01$ Torr) resulted in less than 0.5% of the initial photolysis energy (a maximum of 50 mJ) being absorbed. Furthermore, because of the large bond dissociation energy[24] of $(CN)_2$, about 90% of this energy was used just to dissociate the $(CN)_2$ molecule. The largest perturbation to the gas temperature, at the maximum photolysis laser energy and largest [$(CN)_2$], can be estimated to be only 0.02 K. Much larger uncertainties in the gas temperature arise from the thermal inertia of the inner Teflon box. The TFR apparatus was not designed for very carefully temperature-controlled experiments so that the gas temperature could be different from that recorded by the thermocouples. Five calibrated thermocouples were arranged so that two monitored the temperature of the box near the gas inlet and outlet, two monitored the temperature directly over the photolysis region, and one was suspended directly in the center of the gas stream a few centimeters downstream from the photolysis region, well isolated from the walls. The readings from the two thermocouples directly above the reaction zone and the one directly in the gas stream were always within several kelvin of each other at the highest temperatures, and this was taken as a measure of the uncertainty in the temperature.

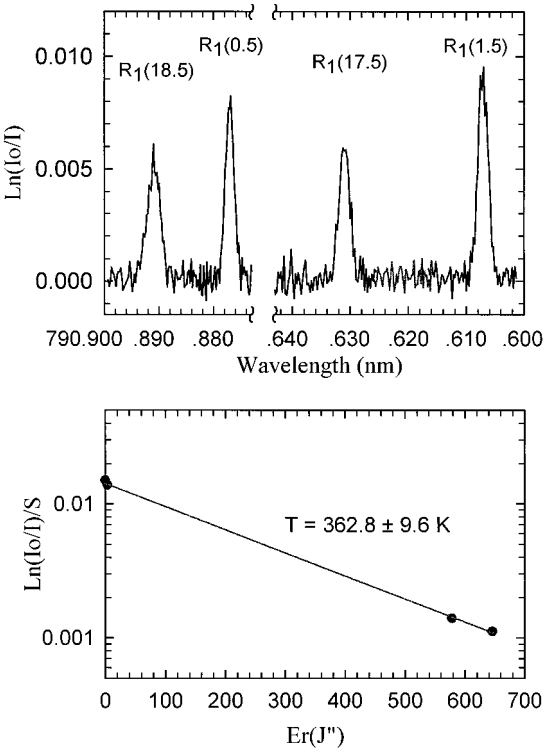

Figure 3. (a) Confirmation that the thermocouples gave the correct gas temperature. A wavelength scan over two pairs of high and low rotational states of CN(v=0) is shown. The measurements were carried out at a total pressure of He of 3.86 Torr. The data were collected with a boxcar delay of 15 μs, and gate width of 1.0 μs and averaged for 30 shots per frequency interval. (b) A Boltzmann plot of the peaks in Figure 3(a), fit to Gaussian profiles, to determine the rotational temperature of the reacting CN radical. The data were normalized for fluctuations in the excimer laser power, *S*. The three thermocouples nearest the reaction zone gave readings of 362.2, 363, and 365 K so there is good agreement between the determination of *T* by the thermocouple and spectroscopic techniques.

To further verified that the gas temperature was correctly given by these three thermocouples, the rotational temperature of the reacting CN was measured directly. The CN $A^2\Pi \leftarrow X^2\Sigma$ (2,0) is especially suited for this purpose because the R_1 bandhead is conveniently located near the peak of the Boltzmann distribution for the temperatures of the experiment, and transitions for both high and low rotational states lie within a small frequency range of each other. A typical scan over several low and high rotational transitions is shown in Figure 3a, and a

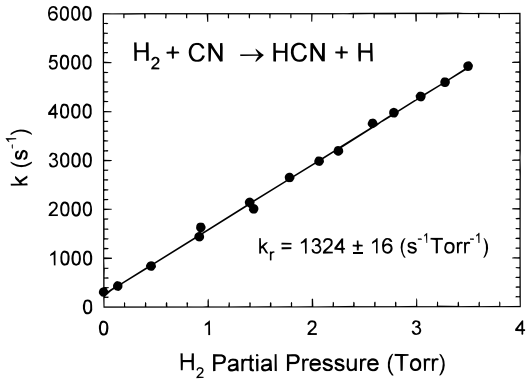

Figure 4. First-order rate constants, as shown in Figure 1(b), are plotted as a function of P_{H_2} for a temperature of 328 K. The diffusion rate of CN in H_2−Ar mixtures was subtracted from each of the first-order decay rates so that the intercept represents the influence of a background reaction of CN. The uncertainty in each first-order rate constant is within the symbols. The linear least-squares fit to the data gives $k_{R1} = (4.5 \pm 0.05) \times 10^{-14}$ (cm^3 $molecule^{-1}$ s^{-1}).

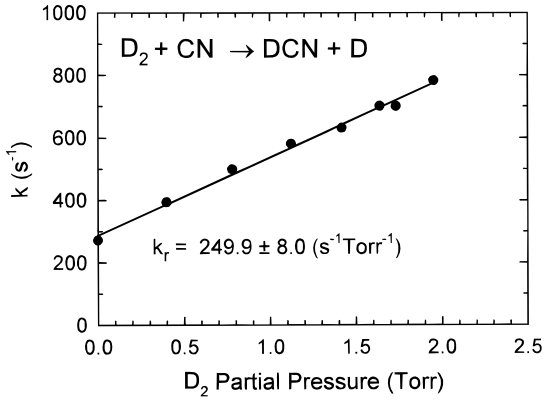

Figure 5. First-order rate constants as shown in Figure 2(b) are plotted as a function of P_{D_2} for a temperature of 293 K. The diffusion rate of CN in D_2 −He mixtures should be approximately independent of the mixture and was not subtracted out from the first-order rate constants so that the intercept contains contributions from diffusion and the CN background reaction. The uncertainty in each first-order rate constant is within the symbols. The linear least-squares fit to the data gives $k_{R2} = (7.6 \pm 0.2) \times 10^{-15}$ (cm^3 $molecule^{-1}$ s^{-1}).

Boltzmann plot of these data is shown in Figure 3b. The slope of the least-squares fit gave a direct measurement of the rotational temperature of the reacting CN radical and was in agreement with the average temperature of the three thermocouples closest to the reaction zone. Other direct measurements of the gas temperature were found to be in good agreement with the average temperature given by these three thermocouple measurements. It was concluded that the gas temperature was well represented by the thermocouple readings with a maximum uncertainty of ±2 K.

The determination of the second-order rate constants by plotting the first-order decay rates as a function of reactant partial pressure minimizes the influence of any impurity on the rate constant determination. As long as an impurity is not introduced along with the variation in the gas flow rates, but arises from a background contamination in the vacuum system, its influence is accounted for by this measurement method. Typical second-order plots for the data sets from which Figures 1 and 2 were taken are shown in Figures 4 and 5, respectively. The nonzero intercept in Figures 4 and 5 indicates that indeed there was a background reaction of CN because k_{CN}^{diff} has been subtracted from the first-order decays, as described. The reaction chamber was not designed to be a high-vacuum apparatus so that a small concentration of impurity could contribute to the removal of CN radicals if the reaction rate constant were large enough, e.g. O_2, $k_{RO_2} = 2.5 \times 10^{-11}$ cm^3 $molecules^{-1}$ s^{-1} at $T = 294$ K.[26] The CN + O_2 reaction could account for a large fraction of the observed intercepts in Figures 4 and 5 if there was a background pressure of ∼1 mTorr of air either due to a vacuum leak or from outgassing. In later experiments, when the diffusion rates of HCN were determined using the infrared laser source, it was discovered that a background reaction produced predominately HCN. Thus, the nature of the apparent background reaction is unclear, but it does not influence the kinetic measurements reported on here. Further discussions of these experiments will be presented in another work.[19]

It is interesting to note that the results reported here were independent of which rotational state of the CN(v=0;J) was monitored. This of course is to be expected because rotational relaxation should proceed much more rapidly than reaction but in many cases has not been verified experimentally.

There could be several possible complications from the photolysis of $(CN)_2$ at 193 nm besides a rise in the gas temperature, namely, the production of electronically and/or vibrationally excited CN products. Fortunately, these effects have been investigated previously. The lowest-lying excited electronic state of CN is the $A^2\Pi$ state, but it is not energetically accessible by a one-photon process at 193 nm.[24] About 13% of the initial CN radicals are produced in the CN(v=1) level.[27,28] However, the presence of CN(v=1) will have little effect on the measurement of the reaction rate constants determined by monitoring CN(v=0). Assuming that the total removal rate for CN(v=1) is larger than that for CN(v=0), the production of CN(v=0) by vibrational relaxation from CN(v=1) would appear as a small rising exponential term in the complete time description of CN(v=0) with a preexponential factor at least 7 times smaller than the term describing CN(v=0) decay. As is evident from Figures 1a and 2a, no such term was detected. Furthermore, previous workers[7,10] have monitored CN(v=1) decay in both the CN + H_2 and D_2 systems and found the decay of CN(v=1) slightly larger than CN(v=0) and attributed this decay to reaction of vibrationally excited CN. A similar conclusion was reached in recent theoretical investigations of reaction R1.[3]

The results for the determination of k_{R1} and k_{R2} are presented in Figures 6 and 7 and summarized in Tables 1 and 2, respectively. A motivating factor in carrying out these experiments was to provide a reliable value for k_{R1} and k_{R2} near room temperature, and a detailed summary of the available data for k_{R1} and k_{R2} is given in Table 3. The average of the rate constants determined in the present experiments at $T = 293$ K is given by $k_{R1} = (2.50 \pm 0.26) \times 10^{-14}$ cm^3 $molecule^{-1}$ s^{-1} and $k_{R2} = (7.5 \pm 0.75) \times 10^{-15}$ cm^3 $molecule^{-1}$ $s.^{-1}$ The error bars include one standard deviation from the average of several measurements at $T = 293$ K and an estimate of a systematic error of ±5% error from determination of the various partial pressures. Near 300 K, the rate constants for the CN + H_2 and D_2 reactions determined in the present work are in good agreement with several recent determinations,[7,8,10,13] and these values are now well established.

As is evident from Figures 1b and 2b, the uncertainty in the determination of each first-order decay rate was quite small; however, the overall scatter in the data was larger than expected considering the excellent signal-to-noise of the individual decay curves. One contributing factor to this scatter is the uncertainty in the gas temperature. Using simple Arrhenius parameters for

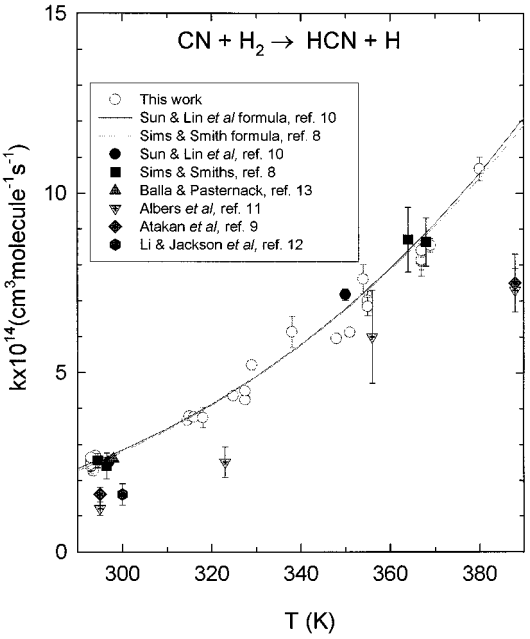

Figure 6. Summary of the available data for the determination of the CN + H_2 reaction rate constant as a function of temperature. The lines are from the fits to the complete data set of Sun et al.[10] and Sims et al.[8] determined over a much wider temperature range. The error bars are all $\pm\sigma$ for the slope to plots such as shown in Figure 4 except for the work of Sims et al.[8] in which the error bars represent $\pm 2\sigma$ and an estimate of systematic errors.

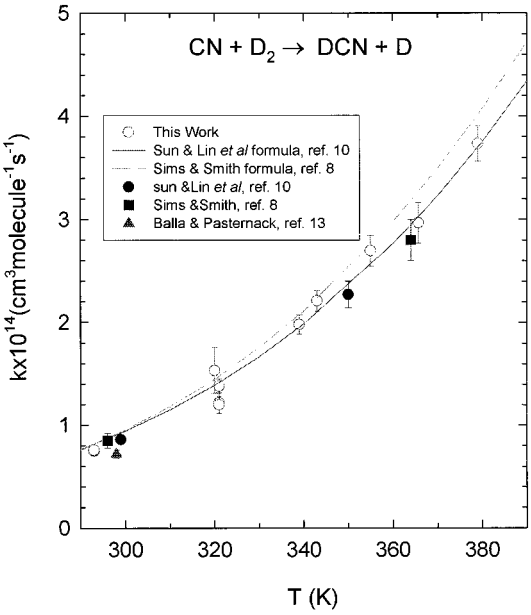

Figure 7. Same as Figure 6 except all the data for the determination of the CN + D_2 reaction rate constant are shown.

this reaction,[8,10] it can be shown that an uncertainty of ± 1 K at 300 K and ± 2 K at 380 K leads to an uncertainty in the rate constant of 2% and 3%, respectively. One systematic trend that was observed was a slight rise in the temperature of the gas mixture with increasing mole fraction of H_2/D_2. Even at the highest temperatures, this effect was small, about a degree, but was unlikely to introduce a systematic error into the data reduction because this effect was within the temperature uncertainty of ± 2 K. In preliminary experiments, it was observed that if sufficient time was not allowed for complete equilibration of the gas mixture throughout the TFR reaction volume, erratic results were obtained. However, in later experiments this effect was eliminated by waiting for a sufficiently long time for the gas to equilibrate. At a total flow rate of 400 sccm the TFR volume was replaced in about a minute. Data were generally collected after waiting at least five pump-out decay times, ensuring that the gas mixture was evenly distributed throughout the TFR volume. No other systematic trends were evident.

TABLE 1: Summary of the Reaction Rate Constant Measurements for the CN + H_2 Reaction

T (K)	carrier gas	P_{tot} (Torr)	$k \times 10^{14}$ (cm^3 molecule^{-1} s^{-1})	± 1 std dev[a]
293	Ar	4.0	2.49	0.12
293	He	4.0	2.38	0.21
293	He	4.0	2.45	0.17
293	He	4.0	2.63	0.11
293	He	3.7	2.51	0.078
293	He	3.7	2.37	0.053
293.5	pure H_2	4.0	2.25	0.019
293.5	Ar	3.6	2.61	0.058
294	He	3.2	2.57	0.047
294	He	5.7	2.48	0.039
294	Ar	3.8	2.60	0.050
294	Ar	4.0	2.68	0.043
314.5	Ar	4.5	3.67	0.05
315	Ar	3.5	3.79	0.033
316	Ar	7.9	3.76	0.056
318	He	4.0	3.74	0.28
325	Ar	3.6	4.35	0.092
327.5	He	3.7	4.24	0.073
327.5	Ar	5.0	4.49	0.054
329	Ar	1.9	5.22	0.14
338	Ar	3.9	6.14	0.44
348	Ar	5.0	5.96	0.083
351	Ar	3.4	6.13	0.098
354	Ar	7.6	7.61	0.40
355	He	4.0	7.02	0.26
355	He	4.0	6.85	0.26
367	He	4.0	8.40	0.19
367	He	3.9	8.10	0.23
367	He	4.0	8.14	0.44
369	He	4.1	8.54	0.19
380	He	4.0	10.7	0.33

[a] $\pm 1\sigma$ uncertainty in the least-squares fit for the slope of k_{CN} vs P_{H_2}.

TABLE 2: Summary of the Reaction Rate Constant Measurements for CN + D_2

T (K)	carrier gas	P_{tot} (Torr)	$k \times 10^{14}$ (cm^3 molecule^{-1} s^{-1})	± 1 std dev[a]
293	He	4.2	0.749	0.028
293	Ar	3.9	0.759	0.024
320	He	4.0	1.53	0.22
321	He	4.2	1.38	0.072
321	He	4.2	1.22	0.10
321	Ar	6.0	1.20	0.083
339	He	4.0	1.98	0.093
343	He	4.0	2.21	0.10
355	He	4.0	2.70	0.15
366	He	3.9	2.97	0.20
379	He	4.0	3.73	0.17

[a] $\pm 1\sigma$ uncertainty in the least-squares fit for the slope of k_{CN} vs P_{D_2}.

The results of this work and other data[7,8,10,13] should provide a reliable database for a comparison with theoretical predictions of the rate constants for the CN + H_2 and D_2 reactions. This in turn will allow for a better theoretical description of this reaction system both in terms of refinements to the PES and also with respect to refinements in the dynamical descriptions leading to rate constant predictions.

The use of direct, long path, time-resolved absorption of CW laser diode radiation is a sensitive method to study the chemical reactions of radicals. The narrow line width, tunability, and

TABLE 3: A Summary of the Measurements for the CN + H_2/D_2 Rate Constants near 300 K

T (K)	technique	$k_{R1} \times 10^{14}$ (cm^3 $molecule^{-1}$ s^{-1})	uncertainty[a] ($\times 10^{14}$)	ref
		CN + H_2		
295	CW abs (B ← X[b])	1.2	0.2	11
300	LIF[c]	1.6	0.3	12
295 ± 4	LIF	2.45	0.5[d]	7
298	IR abs[e]	2.6	0.1	13
294.5	LIF	2.40	0.36[f]	8
296.5	LIF	2.55	0.2[f]	8
295	LIF	1.59	0.17	9
297	LIF	2.51	0.06	10
293 ± 1	CW abs[g] (A ← X)	2.50	0.26[h]	this work
		CN + D_2		
296	LIF	0.85	0.06[f]	8
298	IR abs	0.72	0.4	13
299	LIF	0.86	0.23	10
293 ± 1	CW abs (A ← X)	0.75	0.075[h]	this work

[a] 1σ unless indicated otherwise. [b] CN monitored by time-resolved absorption spectroscopy on the violet B ← X system. [c] CN monitored by LIF using the violet B ← X system. [d] Uncertainty $\pm 2\sigma$. [e] CN monitored by time-resolved infrared absorption spectroscopy on the CN IR fundamental. [f] Uncertainty $\pm 2\sigma$ and an estimate of systematic errors. [g] CN monitored by time-resolved absorption spectroscopy on the red A ← X system. [h] Uncertainty $\pm 1\sigma$ and an estimate of systematic errors.

low-amplitude fluctuation noise of these devices make external cavity CW laser diodes ideal light sources. The narrow line width ensures that even in congested spectral regions absorption features of single rovibrational states can be resolved easily. As well, the narrow line width also ensures that the absorbance is a direct measure of the population in a single rotational state in accordance with the Beer−Lambert law. These laser sources when coupled with high speed and low noise detectors are also capable of measuring reaction rate constants over a wide range of time scales, from 100 MHz to dc. All these attributes are particularly true for the detection of the CN radical using the A ← X (2, 0) transition at 790 nm.

Acknowledgment. The authors wish to thank Dr. A. F. Wagner for many stimulating discussions. This work was supported by the U.S. Department of Energy, Office of Basic Energy Sciences, Division of Chemical Sciences, under contract No. W-31-109-ENG-38.

References and Notes

(1) Bowman, J. M.; Schatz, G. C. *Annu. Rev. Phys. Chem.* **1995,** *46*, 169.
(2) Yang, D. L.; Lin, M. C. In *The Chemical Dynamics and Kinetics of Small Radicals;* Liu, K., Wagner, A. F., Eds.; World Scientific: Singapore, 1996; Part I, Chapter 6.
(3) ter Horst, M. A.; Schatz, G. C.; Harding, L. B. *J. Chem. Phys.* **1996,** *105*, 558.
(4) Che, D.-C.; Liu, K. *Chem. Phys.* **1996,** *207*, 367.
(5) Wang, J.-H.; Liu, K.; Schatz, G. C.; ter Horst, M. *J. Chem. Phys.* **1997**, *107*, 7869.
(6) Wagner, A. F.; Bair, R. A. *Int. J. Chem. Kinet.* **1986,** *18*, 473.
(7) Juan, J.; Smith, I. W. M. *J. Phys. Chem.* **1987,** *91*, 69.
(8) Sims, I. R.; Smith, I. W. M. *Chem. Phys. Lett.* **1988,** *149*, 565.
(9) Atakan, B.; Jacobs, A.; Wahl, M.; Weller, R.; Wolfrum, J. *Chem. Phys. Lett.* **1989,** *154*, 449.
(10) Sun, Q.; Yang, D. L.; Wang, N. S.; Bowman, J. M.; Lin, M. C. *J. Chem. Phys.* **1990,** *93*, 4730.
(11) Albers, E. A.; Hoyermann, K.; Schacke, H.; Schmatjko, K. J.; Wagner, H. G.; Wolfrum, J. *Proceedings of the 15th Symposium (International) on Combustion*; The Combustion Insitute: Pittsburgh, PA, 1974; p 765.
(12) Li, X.; Sayah, N.; Jackson, W. M. *J. Chem. Phys.* **1984,** *81*, 833.
(13) Balla, R. J.; Pasternack, L. *J. Phys. Chem.* **1987,** *91*, 73.
(14) Durant, J. L., Jr,; Tully, F. P. *Chem. Phys. Lett.* **1989,** *154*, 568.
(15) Hall, G. E.; Wu, M. *J. Phys. Chem.* **1993**, *97*, 10911.
(16) North, S. W.; Fei, R.; Sears, T. J.; Hall, G. E. *Int. J. Chem. Kinet.* **1997,** *29*, 127.
(17) Bethardy, G. A.; Northrup, F. J.; Macdonald, R. G. *J. Chem. Phys.* **1995,** *102*, 7966.
(18) Bethardy, G. A.; Northrup, F. J.; He, G.; Tokue, I.; Macdonald, R. G. *J. Chem. Phys.*, submitted for publication.
(19) He, G.; Tokue, I.; Macdonald, R. G. *J. Phys. Chem. A*, in press.
(20) McDaniel, E. W. *Collision Phenomena in Ionized Gases;* John Wiley and Sons: New York, 1964.
(21) Smith, I. W. M.; Warr, J. F. *J. Chem. Soc., Faraday Trans.* **1991,** *87*, 807.
(22) Jeans, J. *An Introduction to the Kinetic Theory of Gases;* Cambridge: London, 1952; Chapter 8.
(23) Berkowitz, J.; Ellison, G. B.; Gutman, D *J. Phys. Chem.* **1994,** *98*, 2744.
(24) Huang, Y.; Barts, S. A.; Halpern, J. B. *J. Phys. Chem.* **1992,** *96*, 425.
(25) Phillips, L. F. *Int. J. Chem. Kinet.* **1978,** *10*, 899.
(26) Smith, I. W. M. In *The Chemical Dynamics and Kinetics of Small Radicals;* Liu, K., Wagner, A. F., Eds.; World Scientific: Singapore, 1996; Part I, Chapter 2.
(27) North, S. W.; Hall, G. E. *J. Chem. Phys.* **1997,** *106*, 60.
(28) Lu, R.; Halpern, J. B.; Jackson, W. M. *J. Phys. Chem.* **1984,** *16*, 3421.